VIP *Porous Coordination Networks*

Zirconium-Metalloporphyrin PCN-222: Mesoporous Metal–Organic Frameworks with Ultrahigh Stability as Biomimetic Catalysts**

Dawei Feng, Zhi-Yuan Gu, Jian-Rong Li, Hai-Long Jiang, Zhangwen Wei, and Hong-Cai Zhou

In nature, metalloporphyrins are well known for performing many biological functions in aqueous media, such as light harvesting, oxygen transportation, and catalysis. Heme, the iron–porphyrin derivative, is the cofactor for many enzyme/ protein families, including peroxidases, cytochromes, hemo-globins, and myoglobins.[1] Using synthetic systems to mimic natural enzymes with high catalytic activity and substrate selectivity has been a sought-after goal in the last decade. Direct application of a heme as an oxidation catalyst in aqueous solution is usually challenging due to the formation of catalytically inactive dimers and catalyst self-destruction in the oxidizing reaction media.[2] One promising approach is to load heme on supports, such as zeolites, clays, nanoparticles, hydrogels, or carbon materials, a practice which inevitably dilutes the density of active sites.[3] An alternative approach is to protect the heme center by modifying the porphyrin to produce dendrimers[4] or molecular crystals,[5] which is a synthetically demanding method. Herein, we propose a unique strategy employing heme-like active centers as structural motifs for the assembly of highly stable porous materials, which should possess well-defined mesochannels and ultrahigh stability in aqueous solution.

Metal-organic frameworks (MOFs) are a new class of crystalline porous materials with fascinating structures and intriguing properties, such as permanent porosity, high surface area, and uniform open cavities.[6] The availability of various building blocks consisting of metals and organic linkers makes it possible to construct MOFs with unique properties for diverse applications.[7] However, these desirable features of MOFs have rarely been applied to an enzymatic mimic, especially for catalysis in an aqueous medium, despite the fact that the assembly of ligands bearing high-density active sites into 3D frameworks may provide an ideal system to both enhance the catalytic activity and protect the cofactors.[8] One

of the main reasons is the lack of water-stable MOFs containing redox-active metal centers.[9] Furthermore, most MOFs are microporous (pore size < 2 nm). Although they are suitable for gas storage, the small pore size slows down diffusion and limits the access of large substrate molecules to the active sites inside a MOF. Therefore, MOFs with mesopores, accessible redox sites, and ultrahigh stability, especially in aqueous media, are indispensible for any successful biomimetic attempt.[10]

Herein we have employed Fe-TCPP (TCPP = tetrakis(4-carboxyphenyl)porphyrin) as a heme-like ligand and chosen highly stable Zr_6 clusters as nodes for the assembly of stable Zr-MOFs. With carefully selected starting materials, we have successfully constructed a 3D heme-like MOF, designated as PCN-222(Fe) (Figure 1; PCN = porous coordination net-
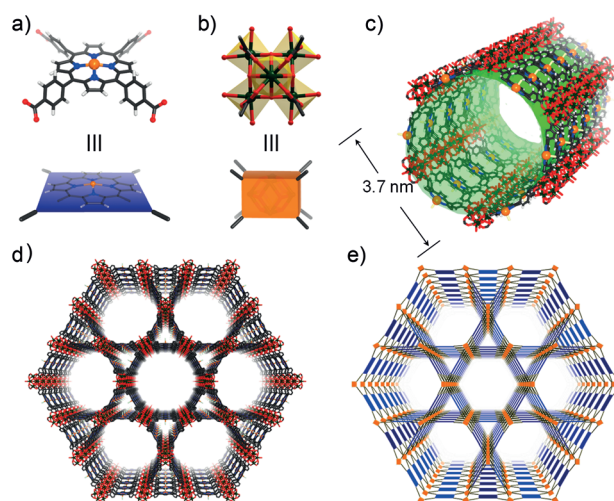

Figure 1. Crystal structure and underlying network topology of PCN-222(Fe). The Fe-TCPP (a; blue square) is connected to four 8-connected Zr_6 clusters (b; light orange cuboid) with a twisted angle to generate a 3D network in Kagome-like topology (d,e) with 1D large channels (c; green pillar). Zr black spheres, C gray, O red, N blue, Fe orange. H atoms were omitted for clarity.

work), which contains one of the largest known 1D open channels, with a diameter of up to 3.7 nm. PCN-222(Fe) also shows exceptional stability, even in concentrated hydrochloric acid. Isostructural MOFs with uncoordinated porphyrin and other metalloporphyrins, including Mn, Co, Ni, Cu, and Zn, have also been produced, affording a new series of stable MOFs. Catalytic studies have demonstrated that PCN-222(Fe) can catalyze the oxidation of a variety of substrates, acting as an effective peroxidase mimic with both excellent

[*] D. Feng,[+] Dr. Z.-Y. Gu,[+] Dr. J.-R. Li, Dr. H.-L. Jiang, Z. Wei,
    Prof. Dr. H.-C. Zhou
    Department of Chemistry, Texas A&M University
    College Station, TX 77843 (USA)
    E-mail: zhou@chem.tamu.edu
    Homepage: http://www.chem.tamu.edu/rgroup/zhou/

    Dr. J.-R. Li
    College of Environmental and Energy Engineering
    Beijing University of Technology
    Beijing, 100124 (P.R. China)

 [+] These authors contributed equally to this work.

substrate binding affinity (K_m) and catalytic activity (k_{cat}), which are superior to hemin in aqueous media.

Solvothermal reactions of M-TCPP (M = Fe, Mn, Co, Ni, Cu, Zn, H$_2$) (50 mg), ZrCl$_4$ (70 mg) and benzoic acid (2.7 g) in *N,N*-dimethylformamide or *N,N*-diethylformamide for 48 h at 120°C yielded needle-shaped single crystals of PCN-222. Single-crystal X-ray diffraction studies revealed that PCN-222(Fe) crystalizes in space group *P6/mmm*. Its framework consists of Zr$_6$ clusters linked by the square planar TCPP ligands. Each Zr$_6$(OH)$_8$ core, in which all of the triangular faces in a Zr$_6$-octahedron are capped by μ$_3$-OH groups (Supporting Information, Figure S4), is connected to eight TCPP ligands. Unlike the the well-known 12-connected Zr$_6$ cluster observed in the UiO-series of MOFs,[11] only eight edges of the Zr$_6$ octahedron are bridged by carboxylates from TCPP ligands in PCN-222, while the remaining positions are occupied by terminal hydroxy groups. Consequently, the symmetry of the Zr$_6$ carboxylate unit is reduced from O_h to D_{4h}, which potentially engenders additional space for the formation of mesopores. The benzene rings of the TCPP ligand also rotate 35.88° from the original position corresponding to that in the free ligands. The 3D framework of PCN-222 can also be viewed as zirconium-carboxylate layers, which form a Kagome-type pattern in the *ab* plane, pillared by TCPP ligands. Remarkably, the 3D framework contains very large hexagonal 1D open channels with a diameter as large as 3.7 nm along the *c* axis, among one of the largest reported in MOFs.[10,12]

The porosity of PCN-222 has been examined by nitrogen adsorption experiments at 77 K. The typical type IV isotherm of PCN-222(Fe) exhibits a steep increase at the point of $P/P_0 = 0.3$, suggesting mesoporosity. A N$_2$ uptake of 1009 cm^{3}g^{-1} (STP) and a Brunauer-Emmett-Teller (BET) surface area of 2200 m^{2}g^{-1} have been observed for PCN-222(Fe), when the activation procedures were carefully optimized by applying a dilute acid solution for pre-activation treatments. The experimental total pore volume of 1.56 cm^{3}g^{-1} is also in good agreement with the calculated pore volume of 1.63 cm^{3}g^{-1}. Evaluation of a density functional theory (DFT) simulation from the N$_2$ sorption curve indicates that there are two types of pores, with sizes of 1.3 nm and 3.2 nm (Figure 2b, inset), assigned to triangular microchannels and hexagonal mesochannels, respectively, which are consistent with the crystallographic data when van der Waals contact is considered. Other PCN-222 MOFs with different porphyrin centers also showed similar type IV N$_2$ sorption isotherms and gave surface area, N$_2$ uptake, and total pore volume of up to 2312 m^{2}g^{-1}, 1067 cm^{3}g^{-1} (STP), and 1.65 cm^{3}g^{-1}, respectively (Supporting Information, Figure S7).

Counter-intuitively, the PCN-222 series possess not only one of the largest open channels, but also extraordinary stability relative to all known MOFs. The powder X-ray diffraction (XRD) patterns remain intact upon immersion in water, boiling water, as well as 2 M, 4 M, 8 M, and even concentrated aqueous HCl solutions for 24 h, suggesting that no phase transition or framework collapse happens during these treatments (Figure 2a). More importantly, the N$_2$ sorption isotherms remained almost the same through all
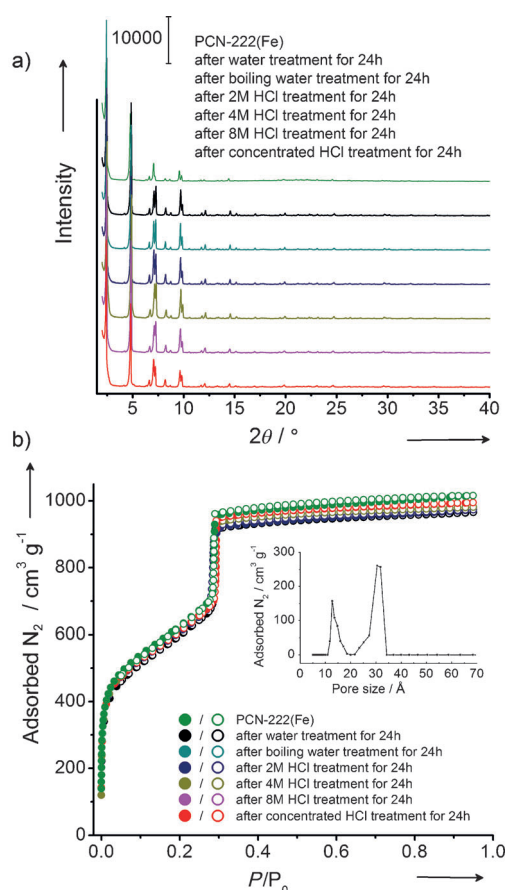

Figure 2. a) Powder X-ray diffraction pattern and b) N$_2$ adsorption isotherms for PCN-222(Fe) at 77 K, showing the framework stability of PCN-222(Fe) upon treatment with water, boiling water, 2 M, 4 M, 8 M, and concentrated HCl. Inset shows DFT pore size distribution for original PCN-222(Fe) using data measured with N$_2$ at 77 K.

treatments, which further confirmed that the tested frameworks remained intact (Figure 2b and Table S4). Strikingly, PCN-222(Fe) survived even after treatment with concentrated HCl, a result which has rarely been observed with MOF materials and which demonstrates its exceptionally high chemical stability. The Zr$_6$ cluster, which was found to be one of the most stable building units for MOF construction, is presumably responsible for the exceptional stability of PCN-222. Zr^{IV}, with its high charge density (Z/r), polarizes the O atoms of the carboxylate groups to form strong Zr–O bonds with significant covalent character. Furthermore, a chelating effect stabilizes the four bonds between Fe^{III} and porphyrin. Therefore, the coordination bonds, and thus the whole framework, become highly resistant to the attack of water and even acid.

PCN-222 is an extraordinary example that meets all the prerequisites for a biomimetic system: ultra-large pore size, exceptionally high water stability, and potentially catalytically active centers. To test the catalytic activity, PCN-222 samples with different metalloporphyrins were employed in the oxidation of several substrates, including pyrogallol, 3,3,5,5-tetramethylbenzidine, and *o*-phenylenediamine (Figure 3a; see also the Supporting Information, Section S10). These oxidation reactions are commonly used standard assays to
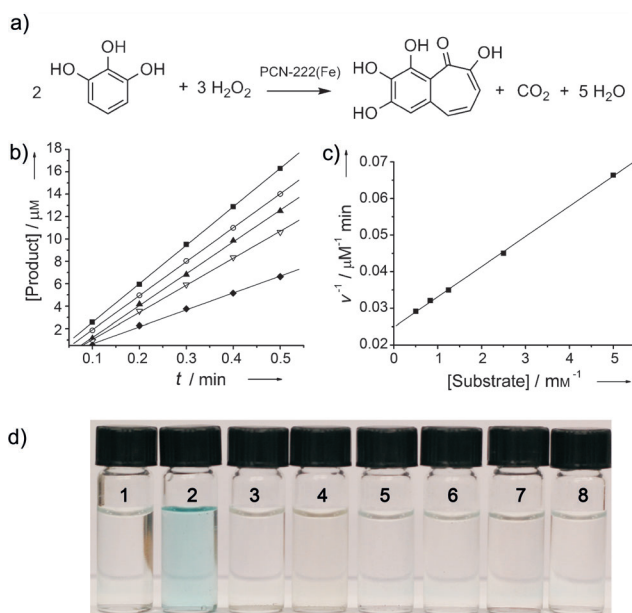
Figure 3. a) Peroxidase-like oxidation reaction of pyrogallol catalyzed by PCN-222(Fe), in which pyrogallol is oxidized to purpurogallin by hydrogen peroxide. b) The initial pyrogallol oxidation profile catalyzed by PCN-222(Fe) (2.5 μM active site equivalent); the concentrations of pyrogallol shown are 0.2 mM (♦), 0.4 mM (▽), 0.8 mM (▲), 1.2 mM (○), and 2.0 mM (■). c) Lineweaver–Burk plot of the pyrogallol oxidation catalyzed by PCN-222(Fe). d) A comparison of the catalytic activities of PCN-222 species in the peroxidase-like oxidation of 3,3,5,5-tetramethylbenzidine (0.7 mM) after one minute. 1: no catalyst, 2: **PCN-222(Fe)**, 3: PCN-222(Mn), 4: PCN-222(Co), 5: PCN-222(Ni), 6: PCN-222(Cu), 7: PCN-222(Zn), and 8: PCN-222(no metal).

Table 1: Kinetic parameters for the oxidation of substrates by different catalysts.

Substrate	Catalyst	K_m [mM]	k_{cat} [min^{-1}]	k_{cat}/K_m [M^{-1}min^{-1}]
pyrogallol	PCN-222(Fe)	0.33	16.1	4.85×10^4
	hemin[3a]	N/A	2.4	N/A
	HRP[3a]	0.81	1.8×10^3	2.20×10^6
3,3,5,5-tetra-methyl-benzidine	PCN-222(Fe)	1.63	14.0	8.59×10^3
	hemin[13]	0.78	0.1	1.26×10^2
	HRP[14]	0.43	2.4×10^5	5.58×10^8
o-phenylene-diamine	PCN-222(Fe)	8.92	7.3	8.18×10^2
	hemin[13]	N/A	0.8	N/A
	HRP[15]	0.14	3.2×10^4	2.37×10^8

N/A = data not available.

characterize the catalytic performance of heme-like enzyme mimics. Kinetic studies revealed that an activated sample of PCN-222(Fe) exhibited excellent peroxidase-like catalytic activity, whereas other MOFs did not show significant activity under identical conditions (Figure 3 d).

These reactions catalyzed by PCN-222(Fe) were carried out with constant hydrogen peroxide and catalyst concentrations (2.5 μM or 10 μM active site equivalent), but with variable substrate concentrations. The reaction process follows the conventional enzymatic dynamic regulation of the Michiaelis–Menten equation, and was monitored by absorption spectroscopy in kinetic mode (Figure 3 b). Based on the different oxidation rates with variable substrate concentrations, a Lineweaver–Burk plot can be obtained with a nearly ideal linear relationship (Figure 3 c), from which important kinetic parameters such as k_{cat} and K_m can be obtained (Table 1). The k_{cat} value, the maximum number of substrate molecules turned over per catalyst molecule per unit time under optimal conditions, gives a direct measure of the catalytic activity. It can also be viewed as the optimum turnover rate. K_m is the Michaelis constant and is often associated with the affinity of the catalyst molecules for the substrate. K_m is also a measure of the substrate concentration required for effective catalysis to occur. For the pyrogallol oxidation reaction, the derived k_{cat} of the PCN-222(Fe) catalyst shows a value of 16.1 min^{-1}, which is seven times higher than the k_{cat} of free hemin (2.4 min^{-1}). Moreover, the

derived K_m value of 0.33 mM for PCN-222(Fe) is lower than that of the natural horseradish peroxidase (HRP) enzyme (0.81 mM), which is indicative of a better affinity of the substrate to PCN-222(Fe). Considering the fast rate of such a catalytic reaction, complete utilization of the porphyrin centers is limited by the diffusion rate of the substrates, which indicates that the actual k_{cat} values of the catalytic centers in PCN-222(Fe) is even higher. Such an excellent catalytic performance can be attributed to the high density of the porphyrin active centers in PCN-222(Fe), which provides one active site per 1286 Da. In sharp contrast, 44174 Da is necessary for each active site in HRP. Other substrates, such as 3,3,5,5-tetramethylbenzidine and o-phenylenediamine, have also been examined for peroxidase-like oxidation to demonstrate the general applicability of PCN-222(Fe) as enzyme mimics. PCN-222(Fe) showed superior catalytic activity to free hemin as the obtained k_{cat} is ranges from nearly ten-times to over two orders of magnitude higher than that of free hemin.

For substrates with different sizes, it is clear that a different level of concentration is required for effective catalysis (K_m). However, it is worth noting that the k_{cat} values for diverse substrates on PCN-222(Fe) are similar, while entirely different catalytic activities for these substrates are observed on hemin and HRP. This observation highlights that PCN-222(Fe) offers large channels with accessible catalytic sites for the substrates, which greatly facilitates their diffusion. The excellent catalytic performance of PCN-222(Fe) is attributed to the successful construction of stable 3D structures with large open channels, which effectively prevents the self-dimerization of porphyrin centers and decreases diffusion resistance. Compared with other MOFs having porphyrin encapsulated in the pores,[9h,i,16] PCN-222, which is constructed with porphyrin struts, and exhibits large mesochannels and high stability, presents a higher density of catalytic centers and faster diffusion rate of substrates, although it may not have specific selectivity for very small-size molecules.

In summary, we have successfully demonstrated a highly stable, mesoporous MOF PCN-222(Fe), which exhibits biomimetic catalytic activities. The active site of the catalyst is located on the inner wall of an open channel with a diameter

of 3.7 nm and shows good activity for the oxidation of a variety of substrates. The integration of a high density of catalytic centers, ultra-large open channels, and the extraordinary chemical stability of PCN-222(Fe) suggests a bright future for building MOF-based platforms for enzyme-mimic catalysis.

Experimental Section

Synthesis of PCN-222: $ZrCl_4$ (70 mg), FeTCPPCl (50 mg) and benzoic acid (2700 mg) in *N,N*-diethylformamide (8 mL) were ultrasonically dissolved in a 20 mL Pyrex vial. The mixture was heated at 120 °C in an oven for 48 h. After cooling down to room temperature, dark brown needle-shaped crystals were harvested by filtration (35 mg, 46 % yield). FTIR (KBr):$\tilde{v}$ = 3381 (m), 2952 (w), 1705 (w), 1601 (s), 1549 (s), 1411 (vs), 1340 (s), 1182 (m), 1003 (s), 871 (w), 809 (m), 776 (m), 723 (s) cm^{-1}. Anal. calcd. (%) for PCN-222(Fe): C, 44.84; H, 2.50; N, 4.36 %. Found: C, 45.59; H, 3.12; N, 4.89 %. PCN-222 with other metalloporphyrin centers were similarly synthesized.

Crystal data from single-crystal diffraction studies for PCN-222 (Fe): $C_{48}H_{32}ClFeN_4O_{16}Zr_3$, $M = 1285.75$, hexagonal, space group $P6/mmm$, $a = b = 41.968(7)$ Å, $c = 17.143(2)$ Å, $V = 26149(7)$ Å^3, $Z = 6$, total reflections = 125 544, independent reflections = 6038, GOF = 1.045, R_1 $[F_0 > 2\sigma(F_0)] = 0.0551$, wR_2 [all data] = 0.1583 (Supporting Information, Section S4).

CCDC 893545 contains the supplementary crystallographic data for this paper. These data can be obtained free of charge from The Cambridge Crystallographic Data Centre via www.ccdc.cam.ac.uk/data_request/cif.

Biomimetic oxidation kinetic studies: The concentration of pyrogallol varies from 0.2–2.0 mM with a fixed concentration of PCN-222(Fe) catalyst (2.5 µM active site equivalent) and a hydrogen peroxide concentration of 50 mM. The catalytic reactions were monitored in kinetic mode at 420 nm with a UV/Vis spectrometer. For other substrates, such as 3,3,5,5-tetramethylbenzidine and *o*-phenylenediamine, similar kinetic assays were performed.

Full experimental details can be found in the Supporting Information.

[1] a) H. B. Dunford in *Encyclopedia of Catalysis*, Wiley, Weinheim, **2002**; b) S. Shaik, S. Cohen, Y. Wang, H. Chen, D. Kumar, W. Thiel, *Chem. Rev.* **2010**, *110*, 949–1017.

[2] T. C. Bruice, *Acc. Chem. Res.* **1991**, *24*, 243–249.

[3] a) Q. Wang, Z. Yang, X. Zhang, X. Xiao, C. K. Chang, B. Xu, *Angew. Chem.* **2007**, *119*, 4363–4367; *Angew. Chem. Int. Ed.* **2007**, *46*, 4285–4289; b) T. Xue, S. Jiang, Y. Qu, Q. Su, R. Cheng, S. Dubin, C.-Y. Chiu, R. Kaner, Y. Huang, X. Duan, *Angew. Chem.* **2012**, *124*, 3888–3891; *Angew. Chem. Int. Ed.* **2012**, *51*, 3822–3825.

[4] M. Shema-Mizrachi, G. M. Pavan, E. Levin, A. Danani, N. G. Lemcoff, *J. Am. Chem. Soc.* **2011**, *133*, 14359–14367.

[5] C. G. Bezzu, M. Helliwell, J. E. Warren, D. R. Allan, N. B. McKeown, *Science* **2010**, *327*, 1627–1630.

[6] H.-C. Zhou, J. R. Long, O. M. Yaghi, *Chem. Rev.* **2012**, *112*, 673–674.

[7] a) P. Horcajada, R. Gref, T. Baati, P. K. Allan, G. Maurin, P. Couvreur, G. Férey, R. E. Morris, C. Serre, *Chem. Rev.* **2012**, *112*, 1232–1268; b) L. E. Kreno, K. Leong, O. K. Farha, M. Allen-dorf, R. P. Van Duyne, J. T. Hupp, *Chem. Rev.* **2012**, *112*, 1105–1125; c) M. P. Suh, H. J. Park, T. K. Prasad, D.-W. Lim, *Chem. Rev.* **2012**, *112*, 782–835; d) K. Sumida, D. L. Rogow, J. A. Mason, T. M. McDonald, E. D. Bloch, Z. R. Herm, T.-H. Bae, J. R. Long, *Chem. Rev.* **2012**, *112*, 724–781; e) M. Yoon, R. Srirambalaji, K. Kim, *Chem. Rev.* **2012**, *112*, 1196–1231; f) Y. Cui, Y. Yue, G. Qian, B. Chen, *Chem. Rev.* **2012**, *112*, 1126–1162; g) J.-R. Li, J. Sculley, H.-C. Zhou, *Chem. Rev.* **2012**, *112*, 869–932; h) H. Wu, Q. Gong, D. H. Olson, J. Li, *Chem. Rev.* **2012**, *112*, 836–868; i) W. Morris, B. Volosskiy, S. Demir, F. Gándara, P. L. McGrier, H. Furukawa, D. Cascio, J. F. Stoddart, O. M. Yaghi, *Inorg. Chem.* **2012**, *51*, 6443–6445; j) W.-G. Lu, C.-Y. Su, T.-B. Lu, L. Jiang, J.-M. Chen, *J. Am. Chem. Soc.* **2006**, *128*, 34–35; k) H.-L. Jiang, Q. Xu, *Chem. Commun.* **2011**, *47*, 3351–3370; l) A. Umemura, S. Diring, S. Furukawa, H. Uehara, T. Tsuruoka, S. Kitagawa, *J. Am. Chem. Soc.* **2011**, *133*, 15506–15513.

[8] J. T. Hupp, *Nat. Chem.* **2010**, *2*, 432–433.

[9] a) B. F. Abrahams, B. F. Hoskins, D. M. Michail, R. Robson, *Nature* **1994**, *369*, 727–729; b) M. E. Kosal, J.-H. Chou, S. R. Wilson, K. S. Suslick, *Nat. Mater.* **2002**, *1*, 118–121; c) M. H. Alkordi, Y. Liu, R. W. Larsen, J. F. Eubank, M. Eddaoudi, *J. Am. Chem. Soc.* **2008**, *130*, 12639–12641; d) A. M. Shultz, O. K. Farha, J. T. Hupp, S. T. Nguyen, *J. Am. Chem. Soc.* **2009**, *131*, 4204–4205; e) R. W. Larsen, L. Wojtas, J. Perman, R. L. Musselman, M. J. Zaworotko, C. M. Vetromile, *J. Am. Chem. Soc.* **2011**, *133*, 10356–10359; f) O. K. Farha, A. M. Shultz, A. A. Sarjeant, S. T. Nguyen, J. T. Hupp, *J. Am. Chem. Soc.* **2011**, *133*, 5652–5655; g) C. Zou, Z. Zhang, X. Xu, Q. Gong, J. Li, C.-D. Wu, *J. Am. Chem. Soc.* **2012**, *134*, 87–90; h) Z. Zhang, L. Zhang, L. Wojtas, M. Eddaoudi, M. J. Zaworotko, *J. Am. Chem. Soc.* **2012**, *134*, 928–933; i) Z. Zhang, L. Zhang, L. Wojtas, P. Nugent, M. Eddaoudi, M. J. Zaworotko, *J. Am. Chem. Soc.* **2012**, *134*, 924–927; j) X.-S. Wang, L. Meng, Q. Cheng, C. Kim, L. Wojtas, M. Chrzanowski, Y.-S. Chen, X. P. Zhang, S. Ma, *J. Am. Chem. Soc.* **2011**, *133*, 16322–16325; k) E.-Y. Choi, L. D. DeVries, R. W. Novotny, C. Hu, W. Choe, *Cryst. Growth Des.* **2010**, *10*, 171–176; l) E.-Y. Choi, C. A. Wray, C. Hu, W. Choe, *CrystEngComm* **2009**, *11*, 553–555; m) P. M. Barron, C. A. Wray, C. H. Hu, Z. Y. Guo, W. Choe, *Inorg. Chem.* **2010**, *49*, 10217–10219; n) E.-Y. Choi, P. M. Barron, R. W. Novotny, H.-T. Son, C. Hu, W. Choe, *Inorg. Chem.* **2009**, *48*, 426–428; o) J. M. Verduzco, H. Chung, C. Hu, W. Choe, *Inorg. Chem.* **2009**, *48*, 9060–9062; p) C. Zou, C.-D. Wu, *Dalton Trans.* **2012**, *41*, 3879–3888.

[10] J. An, O. K. Farha, J. T. Hupp, E. Pohl, J. I. Yeh, N. L. Rosi, *Nat. Commun.* **2012**, *3*, 604.

[11] a) J. H. Cavka, S. Jakobsen, U. Olsbye, N. Guillou, C. Lamberti, S. Bordiga, K. P. Lillerud, *J. Am. Chem. Soc.* **2008**, *130*, 13850–13851; b) A. Schaate, P. Roy, A. Godt, J. Lippke, F. Waltz, M. Wiebcke, P. Behrens, *Chem. Eur. J.* **2011**, *17*, 6643–6651; c) C. Wang, Z. Xie, K. E. deKrafft, W. Lin, *J. Am. Chem. Soc.* **2011**, *133*, 13445–13454.

[12] a) K. Koh, A. G. Wong-Foy, A. J. Matzger, *Angew. Chem.* **2008**, *120*, 689–692; *Angew. Chem. Int. Ed.* **2008**, *47*, 677–680; b) H. Deng, S. Grunder, K. E. Cordova, C. Valente, H. Furukawa, M. Hmadeh, F. Gándara, A. C. Whalley, Z. Liu, S. Asahina, H. Kazumori, M. O'Keeffe, O. Terasaki, J. F. Stoddart, O. M. Yaghi, *Science* **2012**, *336*, 1018–1023.

[13] D. I. Metelitsa, O. B. Rus, A. V. Puchkaev, *Russ. J. Appl. Chem.* **1997**, *70*, 1629–1636.

[14] L. Z. Gao, J. Zhuang, L. Nie, J. B. Zhang, Y. Zhang, N. Gu, T. H. Wang, J. Feng, D. L. Yang, S. Perrett, X. Yan, *Nat. Nanotechnol.* **2007**, *2*, 577–583.

[15] L. V. Bindhu, T. Emilia Abraham, *Biochem. Eng. J.* **2003**, *15*, 47–57.

[16] J. Juan-Alcañiz, J. Gascon, F. Kapteijn, *J. Mater. Chem.* **2012**, *22*, 10102–10118.